Deuteron electroweak disintegration

B. Mosconi
Dipartimento di Fisica, Università di Firenze, Istituto Nazionale di Fisica Nucleare, Sezione di Firenze, I-50125 Firenze, Italy

P. Ricci
Istituto Nazionale di Fisica Nucleare, Sezione di Firenze, I-50125 Firenze, Italy

(Received 26 December 1996)

We study the deuteron electrodisintegration with inclusion of the neutral currents focusing on the helicity asymmetry of the exclusive cross section in coplanar geometry $\mathcal{A}(\vartheta_{\text{c.m.}})$. We stress that a measurement of $\mathcal{A}(\vartheta_{\text{c.m.}})$ in the quasielastic region is of interest for an experimental determination of the weak form factors of the nucleon, allowing one to obtain the parity-violating electron neutron asymmetry. Numerically, we consider the reaction at low-momentum transfer and discuss the sensitivity of $\mathcal{A}(\vartheta_{\text{c.m.}})$ to the strangeness radius and magnetic moment. The problems coming from the finite angular acceptance of the spectrometers are also considered. [S0556-2813(97)01006-6]

PACS number(s): 24.80.+y, 14.20.Dh, 25.10.+s , 25.30.Fj

I. INTRODUCTION

Parity-violating (PV) electron scattering probes weak neutral currents and can provide very interesting information on the strange-quark contributions to the electroweak (ewk) form factors of the nucleon and on the weak-coupling constants at the hadronic level. Since different theoretical models give largely different predictions for the strange vector $[G_E^s(Q^2), G_M^s(Q^2)]$ and axial-vector $[G_A^s(Q^2)]$ form factors as well as for the radiative corrections to the weak-coupling constants, one has to make recourse to an experimental determination of these quantities. For this, one needs to isolate observables which are selectively sensitive to one or the other unknown quantity. It will take a number of measurements in neutrino scattering, PV atomic experiment, and PV electron scattering to determine these form factors and coupling constants. The best information on $G_A^s(Q^2)$ is expected from elastic neutrino scattering experiments where theoretical uncertainties in higher-order processes are small. The BNL experiment 734 [1] already determined a nonzero $G_A^{(s)}(0)$ even if with large errors [2]. Results of the spin-dependent deep inelastic lepton scattering experiments off protons [3–5] and off neutrons [6–9] confirm such a finding, again with large theoretical errors because of the application of SU(3) flavor symmetry to hyperon decays. The LSND experiment on neutrino oscillations [10] presently underway at LAMPF should better constrain $G_A^{(s)}(0)$. The suggestion that the strangeness magnetic moment $\mu_s = G_M^s(0)$ could be determined measuring the PV asymmetry in elastic $\vec{e}p$ scattering at backward angles was put forward by McKeown [11] and Beck [12]. A first experiment [13] aiming to place limits on μ_s is already underway at the Bates Laboratory. Measurements at forward angles could be used to constrain $G_E^s(Q^2)$. The accuracy of such experiments using only a proton target is strongly limited, because of the complications from radiative corrections [14] to the dominant isovector axial-vector coupling. Measuring PV asymmetry in electron scattering from nuclei, where different isospin combinations can be realized, seems a promising way to disentangle radiative corrections and strange-quark contributions. In particular, the PV electron scattering from isoscalar and spinless nuclei, such as ^{4}He, where only the electric weak current can contribute, could lead to a determination of $G_E^s(Q^2)$ [15]. Two experiments of PV electron scattering off complex nuclei have already been carried out [16,17] and several others are in preparation at Bates, CEBAF, and MAMI. For a review we refer to the paper by Musolf *et al.* [18] who present a very detailed discussion of the intermediate-energy semileptonic probes of the hadronic neutral current. Different theoretical approaches have been pursued ranging from the relativistic Fermi gas model [19] to the relativistic mean-field theory [20] to the continuum shell model [21]. Also the case of the deuteron has been studied extensively [22,23].

Up to now, only the helicity asymmetry of the elastic cross section and of the inclusive inelastic cross section in PV electron scattering has been considered [18–20]. In this paper we study the helicity asymmetry of the cross section for the exclusive PV electron deuteron scattering in the in-plane kinematics. In general, namely, in the out-of-plane geometry, the helicity asymmetry is not zero even in the parity conserving (PC) electrodisintegration where it is given by the so-called fifth structure function. Instead, the helicity asymmetry of the in-plane kinematics reaction must vanish in a PC theory. This can be seen using simple geometrical considerations. In fact, the image of the reaction given by a mirror parallel to the scattering plane is the same as the original reaction apart from the change of helicity of the incoming electron. Therefore, if parity is conserved the two processes proceed with equal probability leading to a vanishing asymmetry.

We expect that the obvious drawback of the reduced counting rates of the coincidence experiments might be compensated by the enhanced sensitivity to the form factors of the nucleon detected in coincidence with the electron. In fact, this is the case in the PC electron-deuteron scattering at the quasielastic (QE) peak. It turns out that the deuteron can be confidently used as a quasi-free neutron target in that region.

Therefore, from measurements of $(\vec{e},e'p)$ and $(\vec{e},e'n)$ reactions it should be possible to get information on the isoscalar form factors which take contributions from the strange quark.

We shall neglect the effects of the PV nuclear interactions. In fact, previous studies have shown these PV effects to be small in deuteron photodisintegration [24] as well as in elastic and inelastic electron deuteron scattering [25] except for very low-energy electrons.

In Sec. II we describe our treatment of the PV e-d inelastic scattering and we give the general expression of the helicity asymmetry of the coincidence cross section $\mathcal{A}_p(\vartheta_{\rm c.m.})$. We also discuss its sensitivity to the weak nucleon form factors. In Sec. III we present our numerical results for the exclusive asymmetry in QE kinematics at $Q^2 = 0.1\ (\mathrm{GeV}/c)^{-2}$. Finally, in Sec. IV we state our conclusions.

II. FORMALISM

A. Parity-violating exclusive cross section

The invariant amplitude for the parity-violating exclusive deuteron electrodisintegration, to lowest order, is the sum of the one-photon and the one-Z^0 boson exchange process

$$\mathcal{M}=\mathcal{M}_{[\gamma]}+\mathcal{M}_{[Z^0]}, \tag{2.1}$$

with

$$\mathcal{M}_{[\gamma]}=-4\pi\alpha j_\mu D^{\mu\nu}_{[\gamma]}(Q^2)J^{(\mathrm{em})}_\nu \tag{2.2}$$

and

$$\mathcal{M}_{[Z^0]}=\frac{G}{2\sqrt{2}}M_Z^2(g_V^e j_\mu+g_A^e j_{\mu 5})D^{\mu\nu}_{[Z^0]}(Q^2)J^{(\mathrm{NC})}_\nu, \tag{2.3}$$

where $Q^2=-q_\mu^2>0$ is the four momentum transfer squared, α is the fine-structure constant, G is the weak Fermi constant, M_Z is the Z^0 mass, and g_V^e and g_A^e are the neutral vector and axial-vector couplings of the electron which, in the standard model, are given by $g_A^e=1$, $g_V^e=-1+4\sin^2\vartheta_W\simeq -0.092$, ϑ_W being the Weinberg or weak-mixing angle. The conventions of Musolf *et al.* [18] for the weak-coupling constants are assumed.

The electron vector and axial-vector currents are given by the Dirac form

$$j_\mu=\overline{u(k',s')}\gamma_\mu u(k,s),$$

$$j_{\mu 5}=\overline{u(k',s')}\gamma_\mu\gamma_5 u(k,s), \tag{2.4}$$

where $u(k,s)$ is the electron spinor, (k,s) and (k',s') being the four-momentum and spin of the incoming and outgoing electron, respectively.

As for the hadronic currents, $J^{(\mathrm{em})}$ is the electromagnetic (em) current and $J^{(\mathrm{NC})}$ the neutral current which consists of a vector and an axial-vector component

$$J^{(\mathrm{NC})}=J^{(\mathrm{NC})V}+J^{(\mathrm{NC})A}. \tag{2.5}$$

Finally, the photon propagator is given by

$$D^{\mu\nu}_{[\gamma]}(Q^2)=\frac{1}{Q^2}\left(g^{\mu\nu}+\frac{q^\mu q^\nu}{Q^2}\right), \tag{2.6}$$

in the Landau gauge, while the Z_0 propagator

$$D^{\mu\nu}_{[Z^0]}(Q^2)=\frac{g^{\mu\nu}-q^\mu q^\nu/M_Z^2}{Q^2+M_Z^2}, \tag{2.7}$$

in the limit $Q^2\ll M_Z^2$, which we are interested in, becomes

$$D^{\mu\nu}_{[Z^0]}(Q^2)\simeq\frac{g^{\mu\nu}}{M_Z^2}. \tag{2.8}$$

It is convenient to rewrite the propagators (2.6) and (2.8) in terms of the three polarization vectors $\epsilon^\mu_{(\lambda)}$ $(\lambda=0,\pm1)$ with the properties

$$q_\mu\epsilon^\mu_{(\lambda)}=0, \tag{2.9}$$

$$g_{\mu\nu}\epsilon^{\mu *}_{(\lambda)}\epsilon^\nu_{(\lambda')}=(-1)^\lambda\delta_{\lambda,\lambda'}, \tag{2.10}$$

$$\sum_\lambda(-1)^\lambda\epsilon^{\mu *}_{(\lambda)}\epsilon^\nu_{(\lambda)}=g^{\mu\nu}+\frac{q^\mu q^\nu}{Q^2}. \tag{2.11}$$

If the momentum transfer $\mathbf{q}$ is in the $\hat{z}$ direction the polarization vectors take the form

$$\epsilon^\mu_{(\pm)}=\mp\frac{1}{\sqrt{2}}(0,1,\pm i,0),$$

$$\epsilon^\mu_{(0)}=\frac{1}{Q}(q_{\rm lab},0,0,\omega_{\rm lab}), \tag{2.12}$$

in the laboratory (lab) frame where $q^\mu=(\omega_{\rm lab},0,0,q_{\rm lab})$.

Using the completeness relation (2.11), the propagators can be written as

$$D^{\mu\nu}_{[\gamma]}(Q^2)=\frac{1}{Q^2}\sum_\lambda(-1)^\lambda\epsilon^{\mu *}_{(\lambda)}\epsilon^\nu_{(\lambda)}, \tag{2.13}$$

$$D^{\mu\nu}_{[Z^0]}(Q^2)=\frac{1}{M_Z^2}\left[\sum_\lambda(-1)^\lambda\epsilon^{\mu *}_{(\lambda)}\epsilon^\nu_{(\lambda)}-\frac{q^\mu q^\nu}{Q^2}\right], \tag{2.14}$$

and the invariant amplitude becomes

$$\begin{aligned}\mathcal{M}=&-\frac{4\pi\alpha}{Q^2}\sum_\lambda(-1)^\lambda(j\cdot\epsilon^*_{(\lambda)})(J^{(\mathrm{em})}\cdot\epsilon_{(\lambda)})\\&+\frac{G}{2\sqrt{2}}\sum_\lambda(-1)^\lambda[g_V^e(j\cdot\epsilon^*_{(\lambda)})+g_A^e(j_5\cdot\epsilon^*_{(\lambda)})]\\&\times(J^{(\mathrm{NC})}\cdot\epsilon_{(\lambda)})-\frac{G}{2\sqrt{2}}\frac{1}{Q^2}g_A^e(j_5\cdot q)(J^{(\mathrm{NC})A}\cdot q),\end{aligned} \tag{2.15}$$

where we have applied the continuity equations

$$(j\cdot q)=(J^{(\mathrm{NC})V}\cdot q)=0. \tag{2.16}$$

Clearly expansions (2.13) and (2.14) have allowed us to express the scattering amplitude as the sum of products of separately Lorentz invariant terms (as done by Dmitrasinovic and Gross [26] in the purely em process). In actual calculations we shall evaluate the scalar products involving the electron current in the lab system and those involving the nuclear current in the center of mass (c.m.) system of the outgoing nucleons. Of course, the transformation of $\epsilon^{\mu}_{(\lambda)}$ from the lab frame to the c.m. frame must be taken into account.

The next step is to evaluate $\Sigma_{s'}|\mathcal{M}|^2$, where s' is the spin of the final electron. First of all, we neglect the purely weak component terms, completely negligible being $\sim G^2$. Moreover, we assume, as usual, the extreme relativistic limit (ERL) for the electron ($m_e \ll E_e$). It is straightforward to see that in this limit

$$\sum_{s'} (j\cdot\epsilon^{*}_{(\lambda)})(j^{+}_{5}\cdot q)=0. \tag{2.17}$$

Then, the $\gamma - Z^0$ interference contribution involving the last term of Eq. (2.15) vanishes. This means that the term $\sim q^{\mu}q^{\nu}$ in the Z^0 propagator (2.14) does not contribute and that the γ and Z^0 propagators can be expressed through the completeness relation (2.11) satisfied by the polarization vectors $\epsilon^{\mu}_{(\lambda)}$.

Therefore we obtain

$$\begin{aligned}\sum_{s'} |\mathcal{M}|^2 = {} & \frac{4E_eE_{e'}\cos^2(\vartheta_{e'}/2)}{4m_e^2}\sum_{\lambda\lambda'}(-1)^{\lambda-\lambda'} \\ & \times\left(\frac{q_{\rm c.m.}}{Q}\right)^{2-|\lambda|-|\lambda'|}\left(\frac{4\pi\alpha}{Q^2}\right)^2 \\ & \times\{v^{(VV)}_{\lambda\lambda'}(J^{(\rm em)}\cdot\epsilon_{(\lambda)})(J^{(\rm em)+}\cdot\epsilon^{*}_{(\lambda')}) \\ & - g_{\rm eff}(g^e_V v^{(VV)}_{\lambda\lambda'}+g^e_A v^{(VA)}_{\lambda\lambda'}) \\ & \times[(J^{(\rm em)}\cdot\epsilon_{(\lambda)})(J^{(NC)+}\cdot\epsilon^{*}_{(\lambda')}) \\ & +(J^{(\rm NC)}\cdot\epsilon_{(\lambda)})(J^{(\rm em)+}\cdot\epsilon^{*}_{(\lambda')})]\},\end{aligned} \tag{2.18}$$

where

$$g_{\rm eff}=\frac{Q^2}{4\pi\alpha}\frac{G}{2\sqrt{2}}, \tag{2.19}$$

is the effective weak-coupling constant determining the magnitude of the PV effects in the low and medium Q^2 and $\vartheta_{e'}$ is the electron lab scattering angle.

The electron tensors $v^{(VV)}_{\lambda\lambda'}$, $v^{(VA)}_{\lambda\lambda'}$ which depend on electron kinematic variables only, correspond to the products of vector current-vector current and vector current–axial-vector current. More precisely, they are defined by

$$\begin{aligned}\sum_{s'}(j\cdot\epsilon^{*}_{(\lambda)})(j^{+}\cdot\epsilon_{(\lambda')}) = {} & \frac{4E_eE_{e'}\cos^2(\vartheta_{e'}/2)}{4m_e^2} \\ & \times\left(\frac{q_{\rm c.m.}}{Q}\right)^{2-|\lambda|-|\lambda'|} v^{(VV)}_{\lambda\lambda'}, \\ \sum_{s'}(j\cdot\epsilon^{*}_{(\lambda)})(j^{+}_{5}\cdot\epsilon_{(\lambda')}) = {} & \frac{4E_eE_{e'}\cos^2(\vartheta_{e'}/2)}{4m_e^2} \\ & \times\left(\frac{q_{\rm c.m.}}{Q}\right)^{2-|\lambda|-|\lambda'|} v^{(VA)}_{\lambda\lambda'}.\end{aligned} \tag{2.20}$$

It is straightforward to obtain from Eq. (2.18) the expression of the parity-violating exclusive deuteron electrodisintegration cross section for the polarized electron beam. In terms of the transition matrix elements it reads

$$\begin{aligned}\frac{d^3\sigma}{dE_{e'}d\Omega_{e'}d\Omega^{\rm c.m.}_N} = {} & \frac{1}{3}\frac{\sigma_M}{M_d}\sum_{\lambda\lambda'}\sum_{sm_sm_d}\{v^{(VV)}_{\lambda\lambda'}T^{(\rm em)}_{sm_s\lambda m_d}T^{(\rm em)*}_{sm_s\lambda' m_d} \\ & - g_{\rm eff}(g^e_V v^{(VV)}_{\lambda\lambda'}+g^e_A v^{(VA)}_{\lambda\lambda'}) \\ & \times[T^{(\rm em)}_{sm_s\lambda m_d}T^{(\rm NC)*}_{sm_s\lambda m_d}+T^{(\rm NC)}_{sm_s\lambda m_d}T^{(\rm em)*}_{sm_s\lambda' m_d}]\},\end{aligned} \tag{2.21}$$

where σ_M is the Mott cross section and M_d is the deuteron mass. The superscripts (em) and (NC) indicate to which particular nuclear current the T-matrix element refers to.

The T-matrix elements are related to the hadronic current matrix elements

$$\begin{aligned}T_{sm_s\lambda m_d} = {} & -\sqrt{\frac{p_{\rm c.m.}E^N_{\rm c.m.}E^d_{\rm c.m.}}{16\pi^3}} \\ & \times(-1)^{\lambda}\left(\frac{q_{\rm c.m.}}{Q}\right)^{1-|\lambda|}\langle sm_s|\hat{J}\cdot\epsilon_{(\lambda)}|m_d\rangle,\end{aligned} \tag{2.22}$$

where $\hat{J}$ is the hadronic current operator and the nuclear states are defined in the usual noncovariant normalization; namely $|m_d\rangle$ is the deuteron state normalized to one, with spin projection m_d on the momentum transfer, while the final np state $|sm_s\rangle$, characterized by spin s and its projection m_s on the relative momentum $\mathbf{p}_{\rm c.m.}$, is normalized so that it becomes

$$|sm_s\rangle = e^{i\mathbf{p}_{cm}\cdot\mathbf{r}}\chi_{sm_s}, \tag{2.23}$$

in plane wave (PW) approximation. Of course, in order to calculate the matrix elements in Eq. (2.22), the same quantization axis has to be taken for both initial and final states. This simply amounts to the rotation leading $\mathbf{q}$ into $\mathbf{p}_{\rm c.m.}$ or vice versa. Finally, $E^N_{\rm c.m.}$ and $E^d_{\rm c.m.}$ are the nucleon and deuteron c.m. energy, respectively. Note that, owing to the factorization of (σ_M/M_d) in Eq. (2.21), the T matrix is dimensionless as that introduced in Ref. [27].

Further, we remark that the spherical component $\lambda=0$ of the nuclear current, given in the c.m. frame by

$$J\cdot\epsilon_{(0)}=\frac{q_{\rm c.m.}}{Q}\rho(\mathbf{q})-\frac{\omega_{\rm c.m.}}{Q}(\mathbf{J}\cdot\hat{\mathbf{q}}),\tag{2.24}$$

can be conveniently written in the case of the em current and of the vector component of the neutral current by means of the charge density as

$$J\cdot\epsilon_{(0)}=\left(\frac{Q}{q_{\rm c.m.}}\right)\rho(\mathbf{q}),\tag{2.25}$$

by using the continuity equation to express $(\mathbf{J}\cdot\hat{\mathbf{q}})$ in terms of $\rho(\mathbf{q})$.

In the ERL the electron beam may only have longitudinal polarization of degree h. Therefore, both the electron tensors $v^{(VV,VA)}_{\lambda\lambda'}$ consist of two terms, $v^{(VV,VA)}_{\lambda\lambda'}=v^{(VV,VA)0}_{\lambda\lambda'}+hv^{(VV,VA)h}_{\lambda\lambda'}$ which correspond to unpolarized and polarized electrons, respectively.

It is easy to show that $v^{(VA)}_{\lambda\lambda'}$ are related to the $v^{(VV)}_{\lambda\lambda'}$ in the following way:

$$\begin{aligned}v^{(VA)0}_{\lambda\lambda'}&=v^{(VV)h}_{\lambda\lambda'},\\ v^{(VA)h}_{\lambda\lambda'}&=v^{(VV)0}_{\lambda\lambda'}.\end{aligned}\tag{2.26}$$

Of course, the kinematic functions $v^{(VV)}_{\lambda\lambda'}$ coincide with those $(v_{\lambda\lambda'})$ appearing in parity conserving electron scattering [27,28]. From now on we shall omit any superscript in writing these kinematical functions. We recall that they are symmetric and satisfy the relations

$$\begin{aligned}v_{\lambda\lambda'}&=v_{\lambda'\lambda},\\ v^0_{-\lambda-\lambda'}&=(-)^{\lambda+\lambda'}v^0_{\lambda\lambda'},\\ v^h_{-\lambda-\lambda'}&=(-)^{\lambda+\lambda'+1}v^h_{\lambda\lambda'},\end{aligned}\tag{2.27}$$

induced by parity conservation. Because of Eqs. (2.26) and (2.27) all the possible components of $v_{\lambda\lambda'}$ can be simply derived from the following six components:

$$\begin{aligned}v^0_L&=\zeta^2\xi^2,\\ v^0_T&=\eta+\frac{1}{2}\xi,\\ v^0_{TL}&=\frac{1}{\sqrt{2}}\zeta\xi\sqrt{\eta+\xi},\\ v^0_{TT}&=-\frac{1}{2}\xi,\\ v^h_T&=\sqrt{\eta(\eta+\xi)},\\ v^h_{TL}&=\frac{1}{\sqrt{2}}\zeta\xi\sqrt{\eta},\end{aligned}\tag{2.28}$$

where the indices L, T, TL, and TT correspond to $(\lambda,\lambda')=(0,0)$, $(1,1)$, $(1,0)$, and $(1,-1)$; $\xi=Q^2/q^2_{\rm lab}$ and $\eta=\tan^2(\vartheta_{e'}/2)$. Note that the definitions (2.28) of the $v's$ include the appropriate factors of $\zeta=(q_{\rm lab}/q_{\rm c.m.})$ which are necessary because we calculate the nuclear matrix elements in the c.m. frame.

The cross section (2.21) is the sum of a purely electromagnetic term due to the one-photon exchange process and of the $\gamma-Z^0$ interference term

$$\left(\frac{d^3\sigma}{dE_{e'}d\Omega_{e'}d\Omega^{\rm c.m.}_N}\right)=\left(\frac{d^3\sigma}{dE_{e'}d\Omega_{e'}d\Omega^{\rm c.m.}_N}\right)_{[\gamma]}+\left(\frac{d^3\sigma}{dE_{e'}d\Omega_{e'}d\Omega^{\rm c.m.}_N}\right)_{[\gamma-Z^0]}.\tag{2.29}$$

The dependence of these two terms on the angle ϕ between the reaction plane and the scattering plane can be easily separated out observing that the T-transition matrices depend on ϕ through the phase

$$T_{sm_s\lambda m_d}=e^{i(\lambda+m_d)\phi}t_{sm_s\lambda m_d}.\tag{2.30}$$

The reduced t matrices so defined depend only on the polar nucleon emission angle $\vartheta_{\rm c.m.}$ and on the relative momentum $|\mathbf{p}_{\rm c.m.}|$.

The two cross sections defined in Eq. (2.29) can be written in the form

$$\begin{aligned}\left(\frac{d^3\sigma}{dE_{e'}d\Omega_{e'}d\Omega^{\rm c.m.}_N}\right)_{[\gamma]}&=\frac{\sigma_M}{M_d}(\mathcal{F}+h\mathcal{F}^{(h)}),\\ \left(\frac{d^3\sigma}{dE_{e'}d\Omega_{e'}d\Omega^{\rm c.m.}_N}\right)_{[\gamma-Z^0]}&=\frac{\sigma_M}{M_d}(\mathcal{G}+h\mathcal{G}^{(h)}),\end{aligned}\tag{2.31}$$

where

$$\begin{aligned}\mathcal{G}&=g_{\rm eff}(g^e_V\mathcal{G}_1+g^e_A\mathcal{G}_2),\\ \mathcal{G}^{(h)}&=g_{\rm eff}(g^e_A\mathcal{G}_1+g^e_V\mathcal{G}_2).\end{aligned}\tag{2.32}$$

The functions $\mathcal{F},\mathcal{F}^{(h)},\mathcal{G}_1,\mathcal{G}_2$ are given by

$$\begin{aligned}\mathcal{F}&=v^0_Lf^{(\rm em)}_L+v^0_Tf^{(\rm em)}_T+\cos2\phi v^0_{TT}f^{(\rm em)}_{TT}+\cos\phi v^0_{TL}f^{(\rm em)}_{TL},\\ \mathcal{F}^{(h)}&=\sin\phi v^h_{TL}f^{(\rm em)h}_{TL},\\ \mathcal{G}_1&=v^0_Lf^{(\rm em-V)}_L+v^0_Tf^{(\rm em-V)}_T+v^0_{TL}(\cos\phi f^{(\rm em-V)}_{TL}+\sin\phi f^{(\rm em-A)}_{TL})+v^0_{TT}(\cos2\phi f^{(\rm em-V)}_{TT}+\sin2\phi f^{(\rm em-A)}_{TT}),\\ \mathcal{G}_2&=v^h_Tf^{(\rm em-A)h}_T+v^h_{TL}(\cos\phi f^{(\rm em-A)h}_{TL}+\sin\phi f^{(\rm em-V)h}_{TL}),\end{aligned}\tag{2.33}$$

in terms of the structure functions

$$f^{(\rm em)}_{\lambda\lambda'}=2\left(\frac{1+\delta_{\lambda+\lambda',1}}{1+\delta_{\lambda,0}}\right){\rm Re}(w^{(\rm em)}_{\lambda\lambda'}),\tag{2.34}$$

$$f_{\lambda\lambda'}^{(\mathrm{em})h}=-2\left(\frac{1+\delta_{\lambda+\lambda',1}}{1+\delta_{\lambda,0}}\right)\mathrm{Im}(w_{\lambda\lambda'}^{(\mathrm{em})}),$$

$$f_{\lambda\lambda'}^{(\mathrm{em}-V)}=-2\left(\frac{1+\delta_{\lambda+\lambda',1}}{1+\delta_{\lambda,0}}\right)\mathrm{Re}(w_{\lambda\lambda'}^{(\mathrm{em}-V)}),$$

$$f_{\lambda\lambda'}^{(\mathrm{em}-V)h}=2\left(\frac{1+\delta_{\lambda+\lambda',1}}{1+\delta_{\lambda,0}}\right)\mathrm{Im}(w_{\lambda\lambda'}^{(\mathrm{em}-V)}),$$

$$f_{\lambda\lambda'}^{(\mathrm{em}-A)}=2\left(\frac{1+\delta_{\lambda+\lambda',1}}{1+\delta_{\lambda,0}}\right)\mathrm{Im}(w_{\lambda\lambda'}^{(\mathrm{em}-A)}),$$

$$f_{\lambda\lambda'}^{(\mathrm{em}-A)h}=-2\left(\frac{1+\delta_{\lambda+\lambda',1}}{1+\delta_{\lambda,0}}\right)\mathrm{Re}(w_{\lambda\lambda'}^{(\mathrm{em}-A)}),$$

where

$$w_{\lambda\lambda'}^{(\mathrm{em})}=\frac{1}{3}\sum_{sm_sm_d} t_{sm_s\lambda m_d}^{(\mathrm{em})}t_{sm_s\lambda' m_d}^{(\mathrm{em})*},$$

$$w_{\lambda\lambda'}^{(\mathrm{em}-V)}=\frac{1}{3}\sum_{sm_sm_d} (t_{sm_s\lambda m_d}^{(\mathrm{em})}t_{sm_s\lambda' m_d}^{(\mathrm{NC})V*}+t_{sm_s\lambda m_d}^{(\mathrm{NC})V}t_{sm_s\lambda' m_d}^{(\mathrm{em})*}), \tag{2.35}$$

$$w_{\lambda\lambda'}^{(\mathrm{em}-A)}=\frac{1}{3}\sum_{sm_sm_d} (t_{sm_s\lambda m_d}^{(\mathrm{em})}t_{sm_s\lambda' m_d}^{(\mathrm{NC})A*}+t_{sm_s\lambda m_d}^{(\mathrm{NC})A}t_{sm_s\lambda' m_d}^{(\mathrm{em})*}).$$

The hadronic tensors $w_{\lambda\lambda'}$ satisfy the symmetry relations

$$w_{\lambda\lambda'}^{*}=w_{\lambda'\lambda}, \tag{2.36}$$

$$w_{-\lambda-\lambda'}^{(\mathrm{em})}=(-1)^{\lambda+\lambda'}w_{\lambda\lambda'}^{(\mathrm{em})}, \tag{2.37}$$

$$w_{-\lambda-\lambda'}^{(\mathrm{em}-V)}=(-1)^{\lambda+\lambda'}w_{\lambda\lambda'}^{(\mathrm{em}-V)}, \tag{2.38}$$

$$w_{-\lambda-\lambda'}^{(\mathrm{em}-A)}=(-1)^{1+\lambda+\lambda'}w_{\lambda\lambda'}^{(\mathrm{em}-A)}, \tag{2.39}$$

which have already been used together with Eqs. (2.26) and (2.27) to write Eq. (2.33) in terms of $\lambda=0,1;-\lambda\leqslant\lambda'\leqslant\lambda$ only.

The property (2.36) is an immediate consequence of definitions (2.35). The other properties (2.37)–(2.39) derive from the symmetry relations induced on the t-matrix elements by the parity conservation

$$t_{s-m_s-\lambda-m_d}^{(\mathrm{em}),(\mathrm{NC})V}=(-1)^{1+s+m_s+\lambda+m_d}t_{sm_s\lambda m_d}^{(\mathrm{em}),(\mathrm{NC})V},$$

$$t_{s-m_s-\lambda-m_d}^{(\mathrm{NC})A}=(-1)^{s+m_s+\lambda+m_d}t_{sm_s\lambda m_d}^{(\mathrm{NC})A}. \tag{2.40}$$

The structure function $f_i^{(\mathrm{em})}$ are the usual structure functions of the PC e-d inelastic scattering. The functions $f_i^{(\mathrm{em}-V)}$,$f_i^{(\mathrm{em}-A)}$ are the additional structure functions arising in ewk inelastic scattering from the interference between the em current and the weak vector, axial-vector currents.

Integrating Eq. (2.31) over the outgoing nucleon solid angle, we recover the well-known expression of the inclusive cross section, first given by Walecka [29] on the basis of symmetry considerations and covariance requirement. In such an integration, all the TL and TT interference terms drop to zero and the surviving five exclusive structure functions transform into the inclusive response functions.

B. Nucleon electromagnetic and weak form factors

The general expressions of the matrix elements of the single-nucleon ewk currents consistent with Lorentz covariance and with parity and time-reversal invariance are

$$J_\mu^{(\mathrm{em})}=\frac{1}{2M(1+\tau)}\overline{u(p')}[G_E(p+p')_\mu + G_M(2M\tau\gamma_\mu+i\sigma_{\mu\nu}q^\nu)]u(p), \tag{2.41}$$

$$J_\mu^{(\mathrm{NC})V}=\frac{1}{2M(1+\tau)}\overline{u(p')}[\widetilde{G}_E(p+p')_\mu + \widetilde{G}_M(2M\tau\gamma_\mu+i\sigma_{\mu\nu}q^\nu)]u(p), \tag{2.42}$$

$$J_\mu^{(\mathrm{NC})A}=\overline{u(p')}[\widetilde{G}_A\gamma_\mu+i(\widetilde{G}_P/M)q_\mu]\gamma_5 u(p), \tag{2.43}$$

where M is the nucleon mass, $\tau=Q^2/4M^2$, p and p' are the four-momentum of the incoming and outgoing nucleon, respectively.

In the following, we do not need to care about the induced pseudoscalar current because it does not contribute to observables in PV electron scattering to leading order in ewk coupling. We have chosen the Sachs form of $J^{(\mathrm{em})}$ and $J^{(\mathrm{NC})V}$ because the study of the PC deuteron electrodisintegration has revealed that, unlike the Dirac form of $J^{(\mathrm{em})}$, it leads to nonrelativistic (NR) results close to the full theory results, minimizing the effect of the relativistic corrections. From the same analysis we also know that the cross section is almost insensitive to meson exchange and isobar excitation currents in the QE region. In conclusion we shall not consider relativistic corrections and interaction currents in our calculations.

From the structure of the em and weak-vector current operators in terms of the SU(3)-singlet and -octet currents it follows that the nucleon weak-vector form factors are given by

$$\widetilde{G}_{E,M}(Q^2)=\frac{1}{2}\xi_V^{T=1}G_{E,M}^V(Q^2)\tau_3+\frac{\sqrt{3}}{2}\xi_V^{T=0}G_{E,M}^S(Q^2) + \xi_V^{(0)}G_{E,M}^{(s)}(Q^2), \tag{2.44}$$

with $\tau_3=+1$, -1 for the proton and neutron, respectively. $G_{E,M}^{S(V)}$ is the isoscalar (isovector) combination of the em Sachs form factors, $G_{E,M}^{(s)}$ is the strange-quark contribution, and the couplings are appropriate linear combinations of quark weak-vector charges. In the standard model they have the values

$$\xi_V^{T=1}=2(1-2\sin^2\vartheta_W),\quad \sqrt{3}\xi_V^{T=0}=-4\sin^2\vartheta_W,\quad \xi_V^{(0)}=-1. \tag{2.45}$$

According to [18], we take the strangeness weak vector form factors in the form

$$G_E^{(s)}(Q^2)=\rho_s\tau G_D^V(Q^2)(1+\lambda_E^{(s)}\tau)^{-1},$$
$$G_M^{(s)}(Q^2)=\mu_s G_D^V(Q^2)(1+\lambda_M^{(s)}\tau)^{-1}, \tag{2.46}$$

which is an extension of the Galster parametrization [30] commonly used for the nucleon em form factors

$$G_E^p(Q^2)=G_D^V(Q^2),$$
$$G_E^n(Q^2)=-\mu_n\tau G_D^V(Q^2)(1+5.6\tau)^{-1}, \tag{2.47}$$
$$G_M^p(Q^2)=\mu_p G_D^V(Q^2),\quad G_M^n(Q^2)=\mu_n G_D^V(Q^2),$$

where $G_D^V(Q^2)=(1+Q^2/M_V^2)^{-2}$, with a cutoff mass squared $M_V^2=0.71\ (\mathrm{GeV}/c)^2$.

Expression (2.46) of $G_E^{(s)}$ implements the only theoretical constraint about the strangeness form factors. The nucleon has no net strangeness, so that $G_E^{(s)}(0)=0$ and the low Q^2 behavior of $G_E^{(s)}$ is characterized by the dimensionless strangeness radius

$$\rho_s\equiv\left[\frac{dG_E^{(s)}(Q^2)}{d\tau}\right]_{\tau=0}. \tag{2.48}$$

Also commonly used in the literature is the Dirac strangeness radius

$$r_s^2\equiv-6\left[\frac{dF_1^{(s)}(Q^2)}{dQ^2}\right]_{Q^2=0}. \tag{2.49}$$

Because of the well-known relations between the Sachs and the Dirac form factors, ρ_s, μ_s, and r_s^2 are linearly related by

$$\rho_s=-\frac{2}{3}M^2r_s^2-\mu_s. \tag{2.50}$$

Very little is known about the values of μ_s and r_s^2 even if many calculations of the strangeness vector form factors have been carried out using different approaches (lattice calculations, effective Lagrangian, dispersion relations, hadronic models). The predictions of the strangeness moments are quite different in different approaches and can also largely vary within a given approach because of the need of additional assumptions and approximations. In particular, r_s^2 is predicted to be positive in the dispersion theory analysis of the nucleon isoscalar form factors [31,40], of the same order of magnitude but negative by the chiral quark-soliton model [32] and negative but two orders of magnitude smaller by the kaon-loop calculations [33]. A negative value of r_s^2 is also preferred by the analysis [2] of the $\nu p/\overline{\nu p}$ elastic scattering data [1] which, however, has been criticized for the use of a unique cutoff mass for the three SU(3) axial-vector form factors.

The different existing models widely disagree also about sign and magnitude of μ_s which is predicted to range from $\mu_s=0.4\pm0.3\ \mu_N$ [41] in the chiral hyperbag model to $\mu_s=-0.75\pm0.30\ \mu_N$ [34] using QCD equalities among the octet baryon magnetic moments. Clearly, a model-independent determination of the strangeness moments and, possibly, of the Q^2 dependence of the strangeness form factors, can only come from the experiments.

Analogously to Eq. (2.44), the axial-vector form factor can be decomposed in terms of the third and eighth SU(3) octet components and of the possible strange component

$$\widetilde{G}_A(Q^2)=\frac{1}{2}\xi_A^{T=1}G_A^{(3)}(Q^2)\tau_3+\frac{1}{2}\xi_A^{T=0}G_A^{(8)}(Q^2)$$
$$+\xi_A^{(0)}G_A^{(s)}(Q^2), \tag{2.51}$$

with coupling constants dictated at the tree level by the quark axial charges

$$\xi_A^{T=1}=-2,\quad \xi_A^{T=0}=0,\quad \xi_A^{(0)}=1. \tag{2.52}$$

Note that in this limit the isoscalar component of $\widetilde{G}_A$ fully comes from the strange quark contribution. Information on the $Q^2=0$ value of the SU(3) octet form factors derives from charged current weak interactions. From neutron β decay and strong isospin symmetry it follows $G_A^{(3)}(0)=(D+F)\equiv g_A=1.2601\pm0.0025$ [35], while from hyperon β decays and flavor SU(3) symmetry it follows $G_A^{(8)}(0)=(1/\sqrt{3})(3F-D)=0.334\pm0.014$ [36], D and F being the associated SU(3) reduced matrix elements. The Q^2 dependence of these form factors can be adequately parametrized with a dipole form

$$G_D^A(Q^2)=(1+Q^2/M_A^2)^{-2}, \tag{2.53}$$

with a cutoff mass $M_A=1.032\ \mathrm{GeV}/c$. The same dipole form is suggested in [18] for the strange axial-vector form factor

$$G_A^{(s)}(Q^2)=\eta_s g_A G_D^A(Q^2)(1+\lambda_A^{(s)}\tau)^{-1}. \tag{2.54}$$

Here again, lacking theoretical constraints on $G_A^{(s)}(0)$ and because of the model dependence of the theoretical estimates, values of $\eta_s=G_A^{(s)}(0)/g_A$ have to be extracted from the experiments. As mentioned in the Introduction, the first indications came from the BNL $\nu p/\overline{\nu p}$ experiment and from the EMC data.

As for the weak-coupling constants we emphasize that the values (2.45) and (2.52) are those predicted by the ewk standard model at the tree level. In a realistic evaluation of the amplitude of any electron-hadron process one has to consider the radiative corrections to these values. Such corrections $R_{V,A}^{(a)}$, amounting to a factor $(1+R_{V,A}^{(a)})$ in all the coupling constants except in $\xi_A^{T=0}$ which becomes $\sqrt{3}R_A^{T=0}$, are very difficult to calculate because they receive contributions from a variety of processes (higher-order terms in ewk theory, hadronic physics effects, . . .). They have been estimated by various authors (for a review see Ref. [18], and citations therein) using different approaches and approximations with results in qualitative agreement. More precisely, $R_V^{(a)}$ are estimated to be of the order of a few percent and $R_A^{(a)}$ of the order of some tenth of a percent. Therefore, while $R_V^{(a)}$ can be neglected, the radiative corrections $R_A^{(a)}$ must, in principle, be taken into account.

C. Asymmetry

As said in the Introduction we are interested in the helicity asymmetry of the coincidence cross section, which is defined as

$$\mathcal{A}(\vartheta_{\text{c.m.}},\phi)=\frac{\sigma(h=+1)-\sigma(h=-1)}{\sigma(h=+1)+\sigma(h=-1)}, \qquad (2.55)$$

where $\sigma(h=\pm 1)$ is the exclusive cross section for electrons polarized parallel $(h=+1)$ and antiparallel $(h=-1)$ to their momenta. From Eq. (2.31) we have

$$\mathcal{A}(\vartheta_{\text{c.m.}},\phi)=\frac{\mathcal{F}^{(h)}+\mathcal{G}^{(h)}}{\mathcal{F}+\mathcal{G}}\simeq\frac{\mathcal{F}^{(h)}+\mathcal{G}^{(h)}}{\mathcal{F}}, \qquad (2.56)$$

because $\mathcal{G}$ is negligible with respect to $\mathcal{F}$. The term $\mathcal{F}^{(h)}$ is the purely em contribution to the helicity-dependent part of the cross section (proportional to the fifth structure function $f_{TL}^{(\text{em})h}$) which vanishes in coplanar geometry [see Eq. (2.33)]. Thus, considering the in-plane kinematics and to leading order in G, the helicity asymmetry is given by the interference of weak and em amplitudes and reads

$$\begin{aligned}\mathcal{F}\mathcal{A}(\vartheta_{\text{c.m.}})=g_{\text{eff}}[&g_V^e(v_T^h f_T^{(\text{em}-A)h}\pm v_{TL}^h f_{TL}^{(\text{em}-A)h})\\&+g_A^e(v_L^0 f_L^{(\text{em}-V)}+v_T^0 f_T^{(\text{em}-V)}\pm v_{TL}^0 f_{TL}^{(\text{em}-V)}\\&+v_{TT}^0 f_{TT}^{(\text{em}-V)})], \qquad (2.57)\end{aligned}$$

where the sign $\pm$ corresponds to $\phi=0°,180°$. Note that the z axis is along $\mathbf{q}$ and the y axis is normal to the reaction plane in the direction $\mathbf{k}_e\times\mathbf{k}_e'$.

In an experiment, the finite angular acceptance of the spectrometers makes it unavoidable to also collect nucleons emitted out-of-plane and thus, apparently, to include in the measured asymmetry the effect of the PC contribution $\mathcal{F}^{(h)}$ which could mask the PV asymmetry. Actually, the experimental results correspond to an average of the theoretical expression (2.56) over the spectrometer solid angle. In such an average the influence of the fifth structure function should vanish because $f_{TL}^{(\text{em})h}$ enters the cross section multiplied by a factor $\sin\phi$, if the spectrometer is exactly centered and symmetrical. Since this is not the case in a real experiment, one has to consider the PC asymmetry in the out-of-plane kinematics close to the electron scattering plane. In the next section we shall give a quantitative estimate of how symmetrical the hadron spectrometer must be in order to make possible to extract the PV asymmetry from the measured asymmetry.

The PV exclusive asymmetry (2.57) shows a very rich structure. In fact, it depends on six structure functions which probe different components of the weak vector and axial currents. In principle, the effects of a particular component could be singled out. For example, the longitudinal parts of the weak currents appearing in longitudinal-transverse structure functions $f_{TL}^{(\text{em}-A)h}$ and $f_{TL}^{(\text{em}-V)}$ could be derived from the difference of $\mathcal{A}(\vartheta_{\text{c.m.}})$ measured at the same $\vartheta_{\text{c.m.}}$ in the half-plane $\phi=0°$ and $\phi=180°$. Other structure functions could be isolated by some generalized Rosenbluth decomposition. However, it does not seem to us sensible to further elaborate on this point since such a program is, at the moment, completely beyond experimental feasibility.

To get an idea of how the exclusive asymmetry depends on the weak form factors of the nucleon it is convenient to consider the simplified form of $\mathcal{A}(\vartheta_{\text{c.m.}}=0°)$ obtained in the PWIA model, which consists of taking into account only the dominant contribution arising from the knocked-out nucleon in the plane wave (PW) approximation for the final states and in the S-wave deuteron state. In that approximation, which accurately reproduces the full theory results for nucleons detected in forward direction $(\vartheta_{\text{c.m.}}\simeq 0°)$, one finds

$$\begin{aligned}&\mathcal{A}(\vartheta_{\text{c.m.}}=0°)\\&\simeq -2g_{\text{eff}}\frac{2g_V^e v_T^h\sqrt{\tau}G_M\widetilde{G}_A+g_A^e(v_L^0 G_E\widetilde{G}_E+2v_T^0\tau G_M\widetilde{G}_M)}{v_L^0 G_E^2+2v_T^0\tau G_M^2}.\end{aligned} \qquad (2.58)$$

Therefore, a measurement of the asymmetry for neutrons emitted at $\vartheta_{\text{c.m.}}^n=0°$ or, equivalently, for protons outgoing at $\vartheta_{\text{c.m.}}=180°$, allows one to determine the neutron weak form factors. The difference with the asymmetry in the $\vec{e}d$ inclusive reaction can be easily appreciated recalling the approximate form of the inclusive asymmetry (the so-called static approximation [18]) which is similar to expression (2.58) but depends on the incoherent sum of the contributions coming from the proton and neutron. Thus, while the inclusive asymmetry is sensitive to the average of the nucleon form factors, the exclusive asymmetry feels the influence of the individual form factors. This enhanced sensitivity might make it interesting to measure the exclusive asymmetry not withstanding the reduced rate of the coincidence cross section.

Apart from minor differences deriving from the not completely covariant treatment of the $\vec{e}d$ inelastic scattering, expression (2.58) coincides with the PV electron-free nucleon asymmetry.

Thus, the limiting cases well known from the analysis of the PV $\vec{e}p$ scattering apply in the PV $\vec{e}d$ exclusive disintegration, namely, the magnetic interactions dominate for electrons backwardly scattered, while the electric interactions play a major role for electrons forwardly scattered. The effect of the axial form factor is suppressed because of the small value of the electron weak vector charge, as is already clear in the general expression (2.57).

III. RESULTS

In this paper we limit our considerations to the low-momentum transfer region $[Q^2\simeq 0.1\ (\text{GeV}/c)^2$ as in the SAMPLE experiment] in order to minimize the impact of the uncertainties in the Q^2 dependence of the strange form factors. To be explicit, in the calculations we take the values $\lambda_E^{(s)}=5.6$, $\lambda_M^{(s)}=0$, $\lambda_A^{(s)}=0$ of the parameters which determine the Q^2 fall off in the expressions (2.46) and (2.54) of the strange form factors. Because of the low Q^2 considered, these assumptions should not be crucial.

Furthermore, as reference values for the axial radiative corrections we adopt $R_A^{T=0}=-0.62$ and $R_A^{T=1}=-0.34$ given by Musolf and Holstein [14] using for the hadronic contributions the so-called best estimates for the weak meson-nucleon vertices of Ref. [37]. Finally, we use the value $\eta_s=-0.12$, deduced from the neutrino scattering experi-

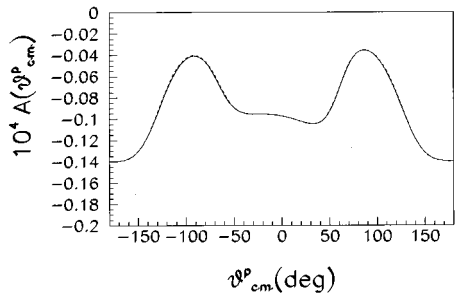

FIG. 1. Angular distribution of the proton asymmetry $\mathcal{A}(\vartheta^p_{\text{c.m.}})$ in the quasielastic region at $Q^2=0.1$ $(\text{GeV}/c)^2$, $\vartheta_e=160°$, with $\mu_s=-0.31\mu_N$, $r_s^2=0.16$ fm^2 [31]. Calculations are with the Paris potential (full line) and the OBEPF potential (dashed line).

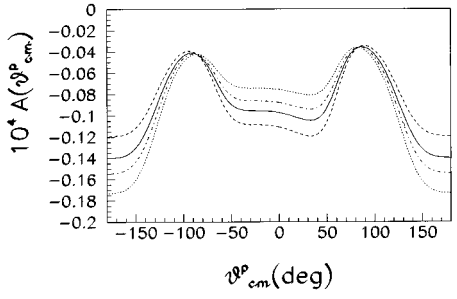

FIG. 2. Dependence of the proton asymmetry $\mathcal{A}(\vartheta^p_{\text{c.m.}})$ on the strange magnetic moment μ_s in the case of $\vartheta_e=160°$. The solid line is the same as in Fig. 1. The other curves are for $\mu_s=-0.75\mu_N$ [34] (dashed line), $\mu_s=0.40\mu_N$ [41] (dotted line), and $\mu_s=0$ (dot-dashed line).

ment, of the strangeness axial charge and, lacking a reliable estimate of the radiative correction to the strangeness axial coupling constant, we take $R_A^{(0)}=0$. Because all the constants entering the calculations, except the strangeness radius and magnetic moment, have been fixed, we can concentrate on the effect of r_s^2 and μ_s on the exclusive asymmetry.

In the following we report the proton asymmetry as a function of the proton polar angles $\vartheta_{\text{c.m.}}$. To distinguish the half-plane $\phi=0°$ and $\phi=180°$, we assign the positive (negative) sign to $\vartheta_{\text{c.m.}}$ for protons emitted in the half-plane $\phi=0°$ ($\phi=180°$). The same figures can be used to deduce the neutron asymmetry $\mathcal{A}_n$, i.e., the PV asymmetry in the $(\vec{e},e'n)$ reaction. Obviously, the value of $\mathcal{A}_n$ for neutrons outgoing at $(\vartheta_{\text{c.m.}},\phi)$ corresponds to the value of the proton asymmetry at $(\pi-\vartheta_{\text{c.m.}},\pi+\phi)$.

Let us start considering the angular distribution of $\mathcal{A}_p(\vartheta_{\text{c.m.}})$ in the QE region for backward scattering electron ($\vartheta_e=160°$), where the role of $G_E^{(s)}$ is strongly suppressed. In Fig. 1 we plot the c.m. angular distribution of $\mathcal{A}_p(\vartheta_{\text{c.m.}})$ calculated with Jaffe's values [31] of the strangeness radius ($r_s^2=0.16$ fm^2) and magnetic moment ($\mu_s=-0.31\mu_N$). In order to study the dependence of the asymmetry on the NN potential models, we have used the deuteron wave functions as well as np continuum wave functions calculated with the Paris potential [38] and with the one boson exchange folded diagram potential OBEPF [39] which gives predictions of the NN data in close agreement with the full Bonn potential. Actually, the final state interactions are taken into account in the multipole amplitudes up to $L=6$, while all the other multipole amplitudes are evaluated in free-wave approximation, as described in Ref. [27]. The angular distribution of $\mathcal{A}_p(\vartheta_{\text{c.m.}})$ is characterized by two minima [note that $\mathcal{A}_p(\vartheta_{\text{c.m.}})$ is negative in all the range of $\vartheta_{\text{c.m.}}$] almost symmetric with respect to **q** and by a maximum at 180°, where the asymmetry is a factor 1.5 higher than at $\vartheta_{\text{c.m.}}=0°$. Obviously such a maximum at backward proton angles corresponds to the emission of neutrons at forward angles.

The very weak dependence on the NN potential model in all the angular ranges suggests some reason beyond the fact that the asymmetry is defined as a ratio of cross sections, which could be the dominance of the transitions from the S-wave deuteron state. The advantage of the exclusive deuteron ewk disintegration which we already have alluded to lies in the possibility of performing simultaneous measurements of $\mathcal{A}_p$ at $\vartheta_{\text{c.m.}}=0°$ and at $\vartheta_{\text{c.m.}}=180°$ or equivalently of $\mathcal{A}_n$ at $\vartheta^n_{\text{c.m.}}=0°$. When combined with the results of the $\vec{e}p$ asymmetry they can lead to an accurate determination of μ_s. The comparison of $\mathcal{A}_p$ at $\vartheta_{\text{c.m.}}=0°$ with the asymmetry in the $\vec{e}p$ scattering should serve as a check of the exclusive experiment.

Intuitively, the exclusive cross section $(e,e'N)$ at the QE peak ($\vartheta^N_{\text{c.m.}}=0°$), where the detected nucleon is ejected in the direction of **q**, should be very close to the cross section for electron scattering on the free nucleon. This is confirmed by actual calculations which give $\mathcal{A}_p=-0.096\times10^{-4}$ and $\mathcal{A}_n=-0.140\times10^{-4}$ with the same choice of form factors and in the same kinematical conditions as in Fig. 1. For comparison, the corresponding values in the $\vec{e}d$ exclusive asymmetry are -0.097×10^{-4} and -0.140×10^{-4}, respectively. This fact will be exploited later on in the discussion of the precision reachable in the determination of μ_s.

The knowledge of $\mathcal{A}_n$ can be exploited directly and through the ratio $\mathcal{A}_p/\mathcal{A}_n$, where the systematic uncertainties cancel to a very large extent since $\mathcal{A}_p$ and $\mathcal{A}_n$ have been measured under exactly the same experimental conditions. A similar cancellation of the systematic errors has been envisaged by the SAMPLE experiment which intends to use the ratio $\mathcal{A}_p/\mathcal{A}_d$, where $\mathcal{A}_d$ is the asymmetry in the inclusive $\vec{e}d$ inelastic scattering.

To show the effect on the asymmetry of variations in the strangeness magnetic moment we report in Fig. 2 our results for the Paris potential and for a selected set of predictions of μ_s. Among the values given by the different models we have chosen those defining the theoretical range of μ_s, i.e., $\mu_s=-0.75$ μ_N [34] and $\mu_s=0.4$ μ_N [41]. Also reported are the curves corresponding to Jaffe's value of μ_s [31] and to $\mu_s=0$. Note that the Dirac strangeness radius has been held fixed at $r_s^2=0.16$ fm^2 as deduced by Jaffe. This comparison makes evident the strong sensitivity on μ_s of the asymmetry for electrons scattered in the backward direction.

To be more quantitative on the precision reachable in a determination of μ_s, let us consider again the PW expression (2.58) of the proton and neutron asymmetry at $\vartheta^N_{\text{c.m.}}=0°$ $(N=p,n)$ and write it in the form

$$\mathcal{A}_N\equiv\mathcal{A}_N^0(1+a_N\rho_s+b_N\mu_s+c_NR_A^{T=1}+d_NR_A^{T=0}+e_N\eta_s), \tag{3.1}$$

TABLE I. Values of the constants entering the expression (3.1) of the proton and neutron asymmetries for $Q^2=0.1$ (GeV/c)^2 and $\vartheta_e=160°$.

	$\mathcal{A}^0$	a	b	c	d	e
proton	-0.88×10^{-5}	-0.16×10^{-2}	-0.342	0.256	-0.072	-0.256
neutron	-0.17×10^{-4}	-0.85×10^{-4}	0.270	0.202	0.057	0.202

which exibits the dependence on the unknown strangeness radius, magnetic moment, and axial charge (in units of g_A) and on the radiative corrections to the axial-vector coupling constant. Actually, the possible modification due to radiative corrections $R_A^{(0)}$ of the strange-quark axial coupling constant is understood in the last term in Eq. (3.1).

The values of $\mathcal{A}_N^0$ and of the other constants are given in Table I. Note, first of all, the smallness of a_N which fully justifies our previous statement about the substantial independence of $G_E^{(s)}$. Second, the influence of $R_A^{T=0}$ is also greatly reduced. Finally, we note that c_N and e_N have the same value and the same sign in the case of the neutron but opposite sign in the case of the proton, as a consequence of our choice $\lambda_A^{(s)}=0$. In fact, in this case we have $e_N=-\tau_3 c_N$. In conclusion, if we further assume that the axial-vector strangeness form factor is known from neutrino scattering experiments [10], the precision $\delta\mu_s$ which can be reached in the determination of μ_s depends on the experimental accuracy in the measurements and on the uncertainty on the isovector axial coupling constant.

Then, from Eq. (3.1) we have that the uncertainty in μ_s together with the error in $R_A^{T=1}$ induce a fractional change in the backward-angle asymmetry given by

$$\frac{\delta\mathcal{A}_{p,n}}{\mathcal{A}_{p,n}}\simeq(b_{p,n}\delta\mu_s+c_{p,n}\delta R_A^{T=1}). \tag{3.2}$$

The $R_A^{T=1}-\mu_s$ correlation is displayed in Fig. 3, where we have assumed an experimental error $\delta\mathcal{A}/\mathcal{A}=\pm7\%$ as in the SAMPLE experiment. The three error bands are for the results on $\mathcal{A}_p$ (full lines), $\mathcal{A}_n$ (dashed lines), and for the ratio $\mathcal{A}_p/\mathcal{A}_n$ (dotted lines). The figure clearly shows that the ratio is almost independent of $R_A^{T=1}$ and this happens because it enters in the proton and neutron asymmetry with the same sign and almost the same value. Clearly, such an experiment allows one to tightly limit the value of μ_s and of $R_A^{T=1}$.

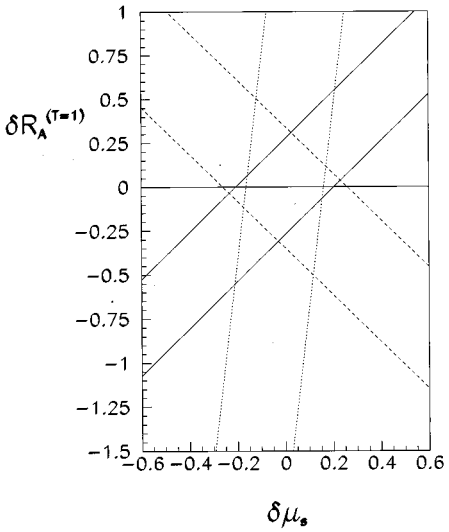

FIG. 3. $(R_A^{T=1}-\mu_s)$ correlation assuming an experimental error $\delta\mathcal{A}/\mathcal{A}=\pm7\%$. The three error bands are for the results on $\mathcal{A}_p$ (full lines), $\mathcal{A}_n$ (dashed lines), and the ratio $\mathcal{A}_p/\mathcal{A}_n$ (dotted lines).

Conversely, once one has determined μ_s and $R_A^{T=1}$, the ratio $\mathcal{A}_p/\mathcal{A}_n$ could be exploited for getting information on the isoscalar part $\tilde{G}_A^{T=0}(Q^2)$ of the axial-vector form factor. In fact, contrary to the isovector part $\tilde{G}_A^{T=1}(Q^2)$, $\tilde{G}_A^{T=0}(Q^2)$ contributes with opposite sign to the proton and neutron asymmetries. Further, if the isoscalar coupling constant $\xi_A^{T=0}$ is assumed to vanish as predicted by the standard model at the tree level so that $\tilde{G}_A^{T=0}(Q^2)$ reduces to the strangeness contribution $G_A^{(s)}(Q^2)$, the effect of the radiative corrections to the strangeness axial-vector coupling constant could be studied.

The exclusive asymmetry $\mathcal{A}_p(\vartheta_{\text{c.m.}})$ is plotted in Fig. 4 in the same kinematical conditions as before, except for the electron scattering angle $\vartheta_e=15°$. In this kinematics, while the effects of the axial current are strongly suppressed because $v_T^h\to0$, those of the electric weak vector current are enhanced $(v_L^0/2v_T^0\to1)$. The asymmetry is calculated with Jaffe's values of μ_s and r_s^2 [31]. Because of its substantial independence of the NN potential models, as seen in Fig. 1, only the results obtained with the Paris potential are drawn.

The sensitivity to the strangeness radius can be appreciated from Fig. 5, where we compare our results of $\mathcal{A}_p(\vartheta_{\text{c.m.}})$ for a restricted selection of predicted r_s^2, all other parameters being the same. Besides that given by Jaffe and $r_s^2=0$, we have used the two almost opposite values $r_s^2=0.21$ fm^2, deduced by Hammer *et al.* [40] in their revised dispersion analysis and $r_s^2=-0.32$ fm^2 obtained by Kim *et al.* [32] (chiral-quark soliton model). At first sight, a measurement of $\mathcal{A}_p(\vartheta_{\text{c.m.}})$ in the forward direction or, better, at $\vartheta_{\text{c.m.}}\sim70°-80°$ where the asymmetry has a maximum,

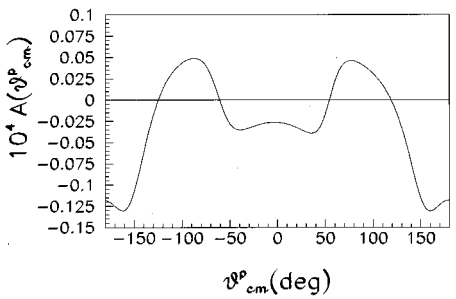

FIG. 4. The same as in Fig. 1 except for $\vartheta_e=15°$. Calculations are with the Paris potential.

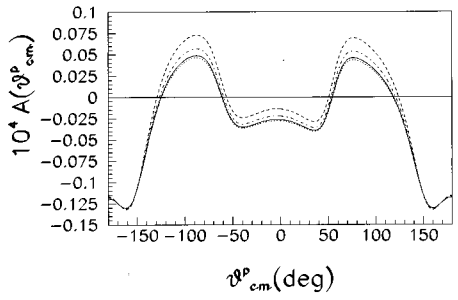

FIG. 5. Dependence of the proton asymmetry $\mathcal{A}(\vartheta^p_{\text{c.m.}})$ on the Dirac strangeness radius r_s^2 in the case of $\vartheta_e=15°$. The solid line is the same as in Fig. 4. The other curves are for $r_s^2=-0.32$ fm^2 [32] (dashed line), $r_s^2=0.21$ fm^2 [40] (dotted line), and $r_s^2=0$ (dot-dashed line).

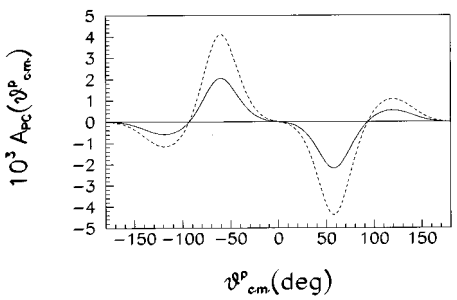

FIG. 6. Angular distribution of the PC proton asymmetry $\mathcal{A}_{\text{PC}}(\vartheta^p_{\text{c.m.}})$ at $Q^2=0.1$ (GeV/c)^2, $\vartheta_e=160°$, for $\phi=2°$ (full line) and $\phi=4°$ (dashed line). Calculations are with the Paris potential.

could lead one to discriminate between the different models. There is no such sensitivity in the asymmetry for neutrons detected at $\vartheta^n_{\text{c.m.}}=0°$, where the asymmetry is a factor 5 higher. The reason is that $\tilde{G}_E^n=0.092G_E^n-G_E^p-G_E^{(s)}$ and G_E^p is so large that variations in $G_E^{(s)}$ cannot be of any importance at low Q^2.

Actually, the precision on the extraction of r_s^2 from such experiment is strongly limited by the error induced by the uncertainty in the other quantities determining $\mathcal{A}_p(\vartheta_{\text{c.m.}})$, and, particularly, in μ_s. In fact, the same considerations of Ref. [42] valid for the $\vec{e}p$ cross-section asymmetry apply to the exclusive $\vec{e}d$ cross-section asymmetry. This can be seen looking at the values of the parameters a_N, b_N reported in Table II. Clearly, the impact of the uncertainty $\delta\mu_s$ on $\delta\rho_s$ is weighted by a large factor, in fact, $b_p/a_p\sim 3.36$, and even worse in the neutron case where $b_n/a_n\sim -49.2$. Also the uncertainty in G_M^n and G_E^n can introduce sizeable errors in $G_E^{(s)}(Q^2)$. As pointed out in [23], the asymmetry of the inclusive $\vec{e}d$ cross section seems more promising for a determination of r_s^2 because the influence of μ_s is suppressed due to the coherent sum of the proton and of the neutron contributions.

Finally, we address the issue of the finite acceptance of the hadron spectrometers, which necessarily leads us to consider the influence of the fifth structure function in the measured asymmetry. Since the typical values of the vertical angular acceptance are $\Delta\phi=\pm 60$ mrad, we have to consider the PC helicity asymmetry $\mathcal{A}_{\text{PC}}(\vartheta^p_{\text{c.m.}})$ in the out-of-plane kinematics, just a few degrees above and below the electron scattering plane.

Similarly to the case of the in-plane kinematics, we report in the same figure the results of $\mathcal{A}_{\text{PC}}(\vartheta^p_{\text{c.m.}})$ corresponding to a full reaction plane, characterizing with positive values of $\vartheta^p_{\text{c.m.}}$ the half-plane ϕ and with negative values of $\vartheta^p_{\text{c.m.}}$ the half-plane $180°+\phi$. The results of $\mathcal{A}_{\text{PC}}(\vartheta^p_{\text{c.m.}})$ reported in Fig. 6 are for the case of backward emitted electrons and for $\phi=2°$ and $4°$. In the calculations of $\mathcal{A}_{\text{PC}}(\vartheta^p_{\text{c.m.}})$ we have also included meson exchange currents of the pionic range and the main relativistic corrections (Darwin-Foldy and spin-orbit terms as well as the wave function relativistic modifications) which have been shown [27] to be sizeable in both the longitudinal-transverse interference structure functions $f_{TL}^{(\text{em})}$ and $f_{TL}^{(\text{em})h}$. The slight asymmetry of $\mathcal{A}_{\text{PC}}(\vartheta^p_{\text{c.m.}})$ in the two half-planes fully comes from the small term proportional to $\cos\phi$ in $\mathcal{F}$. Since $\mathcal{A}_{\text{PC}}(\vartheta^p_{\text{c.m.}})$ is antisymmetric around the electron scattering plane the results of $\mathcal{A}_{\text{PC}}(\vartheta^p_{\text{c.m.}})$ in the half-planes $360°-\phi$ and $180°-\phi$ follow from those in Fig. 6 by a simple change of sign. We can see that, apart from the very forward and backward angles, the size of $\mathcal{A}_{\text{PC}}(\vartheta^p_{\text{c.m.}})$ is some units of 10^{-3}, i.e., two orders of magnitude higher than the PV asymmetry, thus requiring an extremely high level of symmetry in the spectrometers in order to make negligible the PC contributions to the measured asymmetry.

Actually, all our considerations of the coincidence PV asymmetry are for the strict QE peak, i.e., for the region around $\vartheta^p_{\text{c.m.}}=0°$ where the situation is much more favorable because the fifth structure function vanishes at $\vartheta^p_{\text{c.m.}}=0°$, as can be seen in Fig. 7. Here, for typical values $(3°-4°)$ of the horizontal angular acceptance of the spectrometers, the PC asymmetry drops to some units of 10^{-5}. Therefore, if the spectrometers are symmetrical to five parts in 10^4, the PC asymmetry should be cancelled at the 10^{-8} level, thus allowing one to determine the PV asymmetry to a few percent.

The situation is quite similar in the other case considered, i.e., for forward emitted electrons. Here the PC asymmetry is one order of magnitude smaller than in the previous kinematical case but the PV asymmetry is some units of 10^{-6} around $\vartheta^p_{\text{c.m.}}=0°$.

IV. CONCLUSIONS

The aim of this paper was to extend the possible PV observables which could be used for an experimental determi-

TABLE II. The same as in Table I for $\vartheta_e=15°$.

	$\mathcal{A}^0$	a	b	c	d	e
proton	-0.17×10^{-5}	-0.102	-0.343	0.067	-0.019	-0.067
neutron	-0.11×10^{-4}	-0.87×10^{-2}	0.428	0.084	0.024	0.084

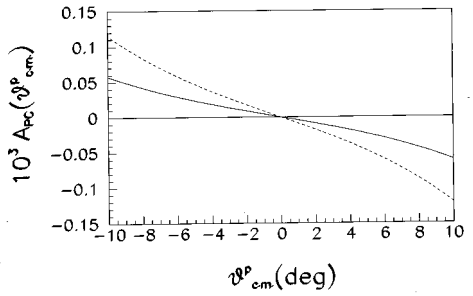

FIG. 7. The same as in Fig. 6 but for the restricted range of the proton emission angle $0° \leqslant \vartheta^p_{\text{c.m.}} \leqslant 10°$.

nation of the weak form factors of the nucleon. To this end we have considered the helicity asymmetry of the $\vec{e}d$ exclusive cross section in the coplanar geometry which, vanishing in the PC theory, directly probes the weak neutral currents.

First of all, we have derived the general expression of the exclusive cross section in the electroweak theory (a result not yet reported in the literature to our knowledge). From this we have deduced the in-plane helicity asymmetry which depends on six structure functions, four of which were derived from the interference of the em current and the weak vector current and two from the interference of the em current and the weak axial current. We have also given an approximate expression of $\mathcal{A}_p(\vartheta_{\text{c.m.}})$ valid at $\vartheta_{\text{c.m.}}=0°$, which allows one to discuss in simple terms the importance of the various weak form factors.

Our expectation that the PV exclusive asymmetry should be of interest for the determination of the strangeness form factors has been confirmed by actual calculations. The point is that the asymmetry of the $\vec{e}d$ exclusive cross section in the QE region allows one to determine the PV asymmetries of both the electron-proton and electron-neutron scattering under the same experimental conditions. Numerically, we have studied such PV asymmetry in the low Q^2 limit in order to minimize the impact of the uncertainty on the Q^2 dependence of the form factors.

We have shown that an experiment with electrons scattered at backward angles could allow one to tightly constrain the value of the strangeness magnetic moment. We have also shown that the asymmetry in the case of forward detected electrons is very sensitive to the strangeness radius. However, the precision in the extraction of ρ_s is rather small because the uncertainties in other quantities, and in particular on μ_s, lead to large errors.

Finally, we have considered the problem connected with the finite angular acceptance of the spectrometers and with their possible asymmetry in the vertical angles, which could lead to the inclusion in the measured helicity asymmetry of some contributions from the PC helicity asymmetry. We have shown that at the QE peak ($\vartheta_{\text{c.m.}}=0°$) the PV asymmetry can be determined to a few percent if the spectrometers are symmetrical to several parts in 10^4.

ACKNOWLEDGMENTS

We thank J. Heidenbauer for providing us with the wave functions corresponding to the OBEPF potential. This work was partly supported by Ministero della Università e della Ricerca Scientifica of Italy.

[1] L.A. Ahrens *et al.*, Phys. Rev. D **35**, 785 (1987).
[2] G.T. Garvey, W.C. Louis, and D.H. White, Phys. Rev. C **48**, 761 (1993).
[3] J. Ashman *et al.*, Phys. Lett. B **206**, 364 (1988); Nucl. Phys. **B328**, 1 (1989).
[4] D. Adams *et al.*, Phys. Lett. B **329**, 399 (1994); **339**, 332(E) (1994).
[5] K. Abe *et al.*, Phys. Rev. Lett. **75**, 25 (1995).
[6] P. Adeva *et al.*, Phys. Rev. B **302**, 533 (1993).
[7] P. Adams *et al.*, Phys. Lett. B **357**, 248 (1995).
[8] P. Anthony *et al.*, Phys. Rev. Lett. **71**, 959 (1993).
[9] K. Abe *et al.*, Phys. Rev. Lett. **74**, 346 (1995).
[10] W.C. Louis, spokesperson, LSND Collaboration, LAMPF proposal Nr. 1173, Los Alamos National Laboratory Report No. LA-UR-89-3764, 1989 (unpublished).
[11] R.D. McKeown, Phys. Lett. B **219**, 140 (1989).
[12] D.H. Beck, Phys. Rev. D **39**, 3248 (1989).
[13] R.D. McKeown and D.H. Beck spokesmen; Bates experiment 89-06 (SAMPLE); E.J. Beise *et al.*, in *Proceedings of the 9th Amsterdam Miniconference on ''Electromagnetic Studies of the Deuteron,''* edited by B. L. G. Bakker, T. Ketel, and H. de Vries (NIKHEF, Amsterdam, 1996), p. 112; E.J. Beise, spokesperson, SAMPLE Collaboration, Report No. nucl-ex/9610011 (unpublished).
[14] M.J. Musolf and B.R. Holstein, Phys. Lett. B **242**, 461 (1990).
[15] M.J. Musolf, R. Schiavilla, and T.W. Donnelly, Phys. Rev. C **50**, 2173 (1994).
[16] P.A. Souder *et al.*, Phys. Rev. Lett. **65**, 694 (1990).
[17] W. Heil *et al.*, Nucl. Phys. **B327**, 1 (1989).
[18] M.J. Musolf, T.W. Donnelly, J. Dubach, S.J. Pollock, S. Kowalski, and E.J. Beise, Phys. Rep. **239**, 1 (1994).
[19] T.W. Donnelly, M.J. Musolf, W.M. Alberico, M.B. Barbaro, A. DePace, and A. Molinari, Nucl. Phys. **A541**, 525 (1992).
[20] C.H. Horowitz and J. Piekarewicz, Phys. Rev. C **47**, 2924 (1993).
[21] J.E. Amaro, J.A. Caballero, T.W. Donnelly, A.M. Lallena, E. Moya de Guerra, and J.M. Udìas, Nucl. Phys. **A602**, 263 (1996).
[22] S. Schramm and C.J. Horowitz, Phys. Rev. C **49**, 2777 (1994).
[23] E. Hadjimichael, G.I. Poulis, and T.W. Donnelly, Phys. Rev. C **45**, 2666 (1992).
[24] E. Hadjimichael and E. Fishback, Phys. Rev. D **3**, 755 (1971).
[25] W.-Y.P. Hwang and E.M. Henley, Ann. Phys. (N.Y.) **129**, 47 (1980); **137**, 378 (1981).
[26] V. Dmitrasinovic and F. Gross, Phys. Rev. C **40**, 2479 (1989).
[27] B. Mosconi and P. Ricci, Nucl. Phys. **A517**, 483 (1990).
[28] B. Mosconi, J. Pauschenwein, and P. Ricci, Phys. Rev. C **48**, 332 (1993).

[29] J.D. Walecka, in *Muon Physics*, edited by V.W. Hughes and C.S. Wu (Academic, New York, 1975), Vol. II, p. 113.
[30] S. Galster, H. Klein, J. Moritz, K.H. Schmidt, D. Wegener, and J. Bleckwenn, Nucl. Phys. **B32**, 221 (1971).
[31] R.L. Jaffe, Phys. Lett. B **229**, 275 (1989).
[32] H-C. Kim, T. Watabe, and K. Goeke, Report No. RUB-TPII-11/95, hep-ph/9506344 (unpublished).
[33] M.J. Musolf and M. Burkhardt, Z. Phys. C **61**, 433 (1994).
[34] D.B. Leinweber, Phys. Rev. D **53**, 5115 (1996).
[35] Particle Data Group, R.M. Barnett *et al.*, Phys. Rev. D **54**, 1 (1996).
[36] F.E. Close and R.G. Roberts, Phys. Lett. B **316**, 165 (1993).
[37] B. Desplanques, J.F. Donoghue, and B.R. Holstein, Ann. Phys. (N.Y.) **124**, 449 (1980).
[38] M. Lacombe, B. Loiseau, J.M. Richard, R. Vin Mau, J. Côté, J. Pirés, and R. De Tourreil, Phys. Rev. C **21**, 861 (1980).
[39] J. Haidenbauer, K. Holinde, and M.B. Johnson, Phys. Rev. C **45**, 2055 (1992).
[40] H.-W. Hammer, Ulf-G. Meissner, and D. Drechsel, Phys. Lett. B **367**, 323 (1996).
[41] S-T Hong and B-Y Park, Nucl. Phys. **A561**, 525 (1993).
[42] M.J. Musolf and T.W. Donnelly, Nucl. Phys. **A546**, 509 (1992); **A550**, 564(E) (1992).